JCTC Journal of Chemical Theory and Computation

pubs.acs.org/JCTC Article

A Unique QP Partitioning and Siegert Width Using Real-Valued Continuum-Remover Potential

Y. Sajeev,* Mushir Thodika, and Spiridoula Matsika

Cite This: *J. Chem. Theory Comput.* 2022, 18, 2863−2874 Read Online

ACCESS | Metrics & More | Article Recommendations | Supporting Information

ABSTRACT: A simple, practical quantum chemical procedure is presented for computing the energy position and the decay width of autoionization resonances. It combines the L^2-stabilized resonance wave function obtained using the real-valued continuum-remover (CR) potential [Y. Sajeev *Chem. Phys. Lett.* **2013**, *587*, 105−112] and the Feshbach projection operator (FPO) partitioning technique. Unlike the conventional FPO partitioning of the total wave function into its resonant $\mathcal{Q}$ *space* and background $\mathcal{P}$ *space* components, an explicit partitioning of the total wave function into its interaction region and noninteraction region components is obtained with the help of real-valued continuum-remover potential. The molecular system is initially confined inside a CR potential which removes the electronic continuum of the molecular system in which its resonance state is embedded and, thus, unravels the $\mathcal{Q}$ *space* component of the resonance wave function as a bound, localized eigenstate of the confined system. The eigenfunctions of the molecular Hamiltonian represented in the $\{1 - \mathcal{Q}\}$ *space* constitute a complementary, orthogonal $\mathcal{P}$ *space*. A unique $\mathcal{QP}$ partition is obtained when the level-shift of the $\mathcal{Q}$ *space* function due to its coupling with the $\mathcal{P}$ *space* is zero, and the resonance width is computed using these unique partitioned spaces. This new procedure, which we refer to as CR-FPO formalism, is formally very simple and straightforward to implement, yet its applications to the resonance state of a model Hamiltonian and to the doubly excited resonance states of atomic and molecular systems at the full-CI level are very accurate as compared to the alternative, very precise L^2 methods. In addition, the CR-FPO formalism is implemented in the multireference configuration interaction (MRCI) method, and uses it for calculating the energy position and the autionization decay width of $^2\Pi_g$ shape resonance in N_2^-.

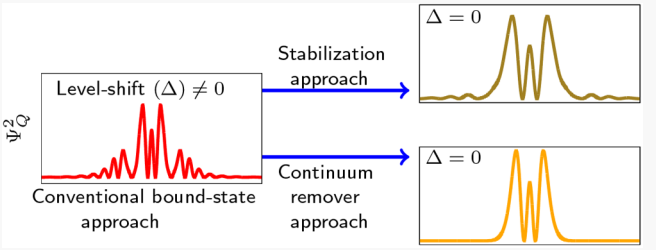

The ability to initiate reaction dynamics through the resonant attachment of low energy electrons (LEE) to molecules has opened up a new and promising line of experimental possibilities for state-specific and site-selective chemical reactions and molecular manipulations.[1−10] The resonant attachment causes fascinating chemistry through the formation of autoionizing transient states, also known as resonance states. The chemical reactions of resonance states play important roles in many areas of research, including radiobiology, astrochemistry and materials chemistry.[11] For example, the negative ion resonance states of biomolecules, which are responsible for long lasting biomolecular damages when the biological cells are exposed to high energy ionizing radiation, are of considerable interest in radiation chemistry.[10,12−16] The vital role of chemical reactions of electronic resonance states in the chemical evolution that occurs in the atmosphere and in the interstellar medium is also being increasingly recognized.[17−19]

As the electronic resonance states have been emerging as a fascinating facet for controlling and catalyzing chemical reactions, direct and easy ways to compute them become more crucial. Because of the transient nature of the resonance states, their direct computation using conventional quantum chemistry methods is not possible.[20] Nevertheless, there has been a tremendous effort to extend the conventionally used bound-state based quantum chemistry approaches, that is, L^2 methods, for computing electronic resonance states.[20−33] The Feshbach projection operator (FPO) formalism[34,35] has been developed as one such method, and has produced excellent results for electronic resonance states of atoms and small molecules.[36−40] However, due to practical challenges, the FPO formalism—although it is very powerful for the description of electronic resonances—has not evolved as a successful approach to exploit all the advancements offered by the bound-state quantum chemistry codes.

In this paper, we report that the FPO formalism becomes completely adaptable to all available *ab initio* many-electron wave function methods for a unique choice of the projectors Q and P, which occur in the formalism. This paper is organized as follows. Section 1 examines the FPO formalism as it is being

Received: November 1, 2021
Published: April 11, 2022

https://doi.org/10.1021/acs.jctc.1c01096
J. Chem. Theory Comput. 2022, 18, 2863−2874

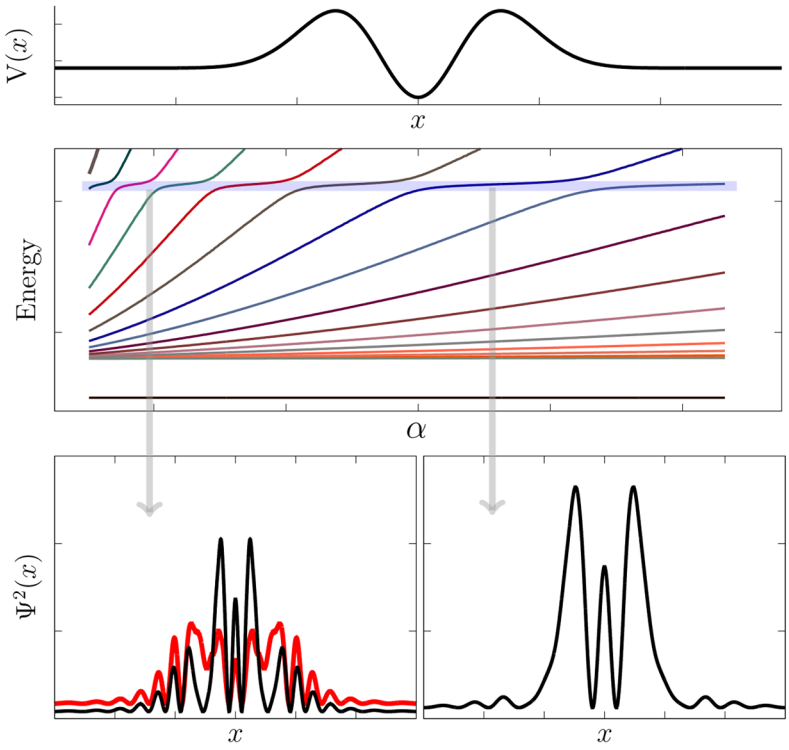

Figure 1. A one-dimensional double barrier potential, which supports an one-electron resonant state, is shown in the top panel. The discrete eigenvalue spectrum of H as a function of the basis set scaling parameter α is shown in the middle panel. The energy position of the resonance is highlighted with a blue background line. The two eigenfunctions that avoid each other and the eigenfunction of the stabilized region are shown, respectively, in the bottom two panels.

developed for an isolated resonance, and reviews the practical difficulties associated with its implementation within the framework of L^2 methods. In section 2, we introduce a new computationally viable FPO formalism. Section 3 illustrates the usefulness and numerical accuracy of the new FPO formalism. Finally, implementation of the new FPO formalism at the multireference level is presented in section 4. Conclusions are given in section 5.

1. FPO FORMALISM FOR THE COMPUTATION OF AN ISOLATED RESONANCE

Here, we shall briefly recall the basic definitions of the FPO formalism for the simplest case, that is, an isolated resonance, that are necessary for introducing our new, improved approach to it. A more detailed discussion of FPO formalism can be found elsewhere (see refs 36−41). The FPO formalism is based on the partitioning of a function space into two subspaces, the resonant $\mathcal{Q}$ *space* and the background scattering $\mathcal{P}$ *space*. Two orthogonal complementary projection operators defined on these subspaces (i.e., Q and P operators), project out the close-in many-body part and the background scattering continuum part of the total resonance wave function.

$$H(Q\Psi + P\Psi) = E\Psi \tag{1}$$

Operating from the left with Q and P, respectively, the Schrödinger equation yields two coupled equations

$$H_{QQ}\Psi_Q + H_{QP}\Psi_P = E\Psi_Q \tag{2a}$$

$$H_{PP}\Psi_P + H_{PQ}\Psi_Q = E\Psi_P \tag{2b}$$

where, in the shorthand notations, $\Psi_Q = Q\Psi$, $\Psi_P = P\Psi$, $H_{PP} = PHP$, $H_{PQ} = PHQ$, etc. Equations 2a and 2b can be formally decoupled by eliminating Ψ_Q to obtain an explicit effective operator equation for Ψ_P

$$\Psi_Q = (E - H_{QQ})^{-1}H_{QP}\Psi_P \tag{3a}$$

$$[H_{PP} + H_{PQ}(E - H_{QQ})^{-1}H_{QP} - E]\Psi_P = 0 \tag{3b}$$

For an isolated resonance (i.e., $Q = |\Psi_Q\rangle\langle\Psi_Q|$, and Ψ_Q is an eigenfunction of H_{QQ} with eigenvalue E_Q), eq 3b can be written as

$$(H_{PP} - E)\Psi_P = -\frac{H_{PQ}|\Psi_Q\rangle\langle\Psi_Q|H_{QP}}{E - E_Q}\Psi_P \tag{4}$$

Letting χ_E to be a solution of the homogeneous equation

$$(H_{PP} - E)\chi_E = 0 \tag{5}$$

eq 4 can be solved using the spectral representation of the standing-wave Greens' function for eq 5. By comparing the solution of eq 4 to the Breit-Wigner resonance formula, the width of an isolated resonance decaying into a single open channel is obtained as

$$\Gamma(E) = 2\pi|\langle\Psi_Q|H_{QP}|\chi_E\rangle|^2 \tag{6}$$

$\Gamma(E)$ is related to the local Siegert decay width

$$\Gamma = \Gamma(E_{res}) \tag{7}$$

where resonance energy, E_{res}, is given by

$$E_{res} = E_Q + \Delta = E_Q + \langle\Psi_Q|H_{QP}(E_{res} - H_{PP})^{-1}H_{PQ}|\Psi_Q\rangle \tag{8}$$

https://doi.org/10.1021/acs.jctc.1c01096
J. Chem. Theory Comput. 2022, 18, 2863−2874

Starting with the FPO formalism, and as discussed formally by O'Malley, the most simple and practical approach for an isolated resonance state of a many-electron system would be to obtain an explicit $\mathcal{QP}$-partitioned representation of H.[38]

$$\mathbf{H} = \left(\begin{array}{c|cccc} E_Q & H_{QP_1} & H_{QP_2} & \cdots & H_{QP_n} \\ \hline H_{P_1Q} & E_{P_1} & 0 & \cdots & 0 \\ H_{P_2Q} & 0 & E_{P_2} & \cdots & 0 \\ \vdots & \vdots & \vdots & \ddots & 0 \\ H_{P_nQ} & 0 & 0 & \cdots & E_{P_n} \end{array}\right) \quad (9)$$

The state Ψ_Q representing resonance is only an approximate eigenfunction of H; resonance decay occurs because of the off-diagonal coupling elements H_{PQ}.

Practical Difficulties in Implementing FPO Formalism within the Bound-State Methods. In principle, a partitioned matrix representation of H can be easily obtained using conventional quantum chemical methods. Unfortunately, resonance solutions are not possible to obtain directly from such partitioned matrices. To illustrate the underlying practical difficulties for the direct computation of resonance solutions from such partitioned matrices, here we briefly consider the stabilization method applied for the resonance solutions of a one-electron model Hamiltonian. A stabilization plot is obtained when the discrete continuum eigenvalues are plotted as a function of the stabilization parameter, for example, the scaling factor α for the exponents of the basis set.[25,26,31] A resonance is revealed in a stabilization plot as a pattern of energy stabilization conjoined with avoided crossings. See Figure 1, where a typical stabilization plot, which is obtained for an one-electron model Hamiltonian is shown. The numerical details of this one-electron problem will be discussed in section 3.

The discrete eigenvalue spectrum of H represented in a standard L^2 basis set may either belong to the stabilized region or to the avoided crossing of the stabilization plot. Although the resonance wave function is uniquely defined by its energy in the stabilized region, the convenience of this uniqueness cannot be directly exploited in the FPO formalism as the $\mathcal{QP}$ separability is not intrinsic to the discrete spectrum corresponding to the stabilized region. This is because the eigenfunction belonging to the stabilized region is an approximation to the total wave function Ψ.

In contrast to the stabilized region, the $\mathcal{QP}$ separability of eigenfunctions is natural in the avoided crossings. Ideally, Ψ_Q is one of the two discrete eigenfunctions of the avoided crossing whose energy is close to E_{res}. The $\mathcal{P}$ *space* can be easily constructed as follows. The physical Hamiltonian H is rediagonalized in the $\{1 - Q\}$*space* and for a different α value. The eigenfunctions of this rediagonalization constitute the $\mathcal{P}$ *space*. Although the computational complexity is aggravated by the use of two different α values, that is, one for Q *space* and one for $\mathcal{P}$ *space*, it ensures the coupling between H_{PP} and H_{QQ}, and yields a partitioned representation of the physical Hamiltonian as shown in eq 9. However, the ability of the discrete continuum solution χ_n of the H_{PP} block to represent χ_E poses serious practical difficulties.

The function χ_E in eq 6 is an energy normalized scattering function representing the background continuum at energy E. The conventional bound state quantum chemistry codes are inadequate for the explicit computation of χ_E with correct energy normalization, which is one of the crucial conditions for numerical computation of decay width. A discrete continuum solution χ_n computed using bound-state code can approximate χ_E when $E = \epsilon_n$, except for an overall normalization factor because χ_n is unit-normalized, whereas χ_E is energy normalized. Nevertheless, there are many nontrivial theoretical developments for computing a continuous approximation for Γ when the calculations are performed in an L^2 basis set, for example, Stieltjes-moment-theory techniques and Gauss quadrature approaches.[36,42] This by no means exhausts the quest for the development of new practical approaches that avoids the explicit computation of χ_E or employing a continuous approximation for Γ.

2. OUR METHOD: CR-FPO FORMALISM

Resonant-Background vs Inner-Outer Based $\mathcal{QP}$ Partitioning. The stabilized region is computationally very appealing due to its unique energy. As we discussed above, the eigenfunctions in the stabilized region, however, are inadmissible to *resonant-background* based QP-partitioning. In the resonant-background based $\mathcal{QP}$ partitioning, the projected wave functions are imperative to the asymptotic conditions

$$\lim Q\Psi = \lim \Psi_Q = 0 \quad \text{as } r \to \infty \quad (10)$$

$$\lim P\Psi = \lim \Psi_P = \Psi \quad \text{as } r \to \infty \quad (11)$$

By restraining eq 11, alternate definitions of partitioning are permitted by the FPO formalism.[37] Here, we propose new requisites for the $\mathcal{QP}$ separability in the stabilized region.

An explicit partitioning of the physical space into the *inner* interaction region and *outer* noninteraction region appears to be an inexpensive way of obtaining a new asymptotic condition and a new $\mathcal{QP}$ separability for the stabilized region. Therefore, we modify the stabilization procedure, which we will soon discuss, for the following explicit *inner*−*outer* partitioning conditions

$$\lim Q\Psi = \lim \Psi_Q^m \cong \Psi \quad \text{inner} \quad (12)$$

$$\lim Q\Psi = \lim \Psi_Q^m = 0 \quad \text{outer} \quad (13)$$

$$E_{res} \cong (E_Q = \langle \Psi_Q^m | H | \Psi_Q^m \rangle) \quad (14)$$

where the superscript "m" stands for our modified stabilization procedure, Ψ_Q^m is the new stabilized wave function, and we assume that the total energy is obtained solely from the many-body effects in the interaction region of the Hamiltonian. A unitary transformation of the $\{1 - Q\}$ *space* yields us the $\mathcal{P}$ *space* that allows the decay of Ψ_Q^m from the *inner* region to the *outer* region.

Construction of $\mathcal{QP}$-Partitioned Representation of *H*. There is no straightforward approach in the conventional quantum chemistry method to obtain an *inner*−*outer* based $\mathcal{QP}$ partitioning and the partitioned representation of H, as given in eq 9. Therefore, a systematic restructuring of the conventional quantum chemistry methods is necessary. In our approach, an explicit *inner*−*outer* based $\mathcal{QP}$-partitioned matrix representation of H is achieved in the conventional quantum chemistry framework through the following steps.

Step 1: Computation of Ψ_Q^m and $\{1 - Q\}$ *space*.

The completeness of the basis set inside the interaction region is essential to obtain Ψ_Q^m that satisfies eq 12. A practical approach to accomplish the completeness of the basis functions inside the interaction volume is to saturate a standard Gaussian basis set

https://doi.org/10.1021/acs.jctc.1c01096
J. Chem. Theory Comput. 2022, 18, 2863−2874

with a set of even-tempered Gaussian primitives. However, if such a saturated set is employed, the application of the Rayleigh-Ritz variational principle to compute Ψ_Q^m state of a many-electron system will collapse to its discrete continuum representations.[43]

The real-valued continuum remover (CR) method, which we proposed in 2013, offers the calculation of Ψ_Q^m using saturated basis sets.[43] Here, the asymptotic one-body potential of H, that is, the noninteraction region of H, is modified using an artificial real-valued confinement potential.

$$\hat{H}^m = \hat{H} + \sum_{i}^{\text{all electrons}} \hat{W}_i \tag{15}$$

As a result of the confinement, the many discrete continuum representations of Ψ_Q^m are removed in the eigenvalue spectrum of H^m and, therefore, the name continuum remover potential. Here, Ψ_Q^m is directly obtained as a localized, bound state eigenfunction of H^m and satisfies eq 12. Therefore, it is also an easy way to achieve an explicit *inner−outer* based $\mathcal{QP}$ partitioning in practical calculations.

We have been using asymptotically defined quadratic potential of the form

$$\hat{W} = \hat{W}(x) + \hat{W}(y) + \hat{W}(z) \tag{16}$$

$$\hat{W}(\varsigma) = \begin{cases} \lambda(\varsigma_o + |\varsigma|)^2, & |\varsigma| > \varsigma_o \\ 0, & |\varsigma| \le \varsigma_o \end{cases} \tag{17}$$

as the continuum remover confinement potential, where λ is the strength of the potential and ς_o is the asymptotic region at which the potential is turned on to a nonzero value. A numerically integrable form of this potential is also in use.

$$\hat{W}(\varsigma) = \lambda\varsigma^2[1 - 0.5(\tanh(\varsigma + \varsigma_o) - \tanh(\varsigma - \varsigma_o))] \tag{18}$$

In preference to the infinite well potential, one may use a finite well potential which can shift the autoionization threshold above the resonance state

$$\hat{W}(\varsigma) = \frac{d}{2}\left[1 - \frac{\tanh(\varsigma + \varsigma_o)}{(1 + e^{\varsigma})} - \frac{\tanh(\varsigma - \varsigma_o)}{(1 + e^{-\varsigma})}\right] \tag{19}$$

where the d is the depth of the well potential. For the sake of convenience, we label the two variants of the CR potentials given in eq 18 and eq 19 (see Figure 2) as CR-A and CR-B, respectively. Most importantly, these variants of the CR potentials can be used in conjunction with all the L^2-based quantum chemical method with relatively modest computational effort and, therefore, all the quantum chemical techniques developed for the bound state problem are also immediately available to the computation of Ψ_Q^m. One may note that, as in the spirit of the continuum-remover potential used here, one-electron artificial shift potentials were used earlier for separating the resonance states from the underlying continuum.[44,45] Unlike these potentials, the form of the continuum-remover potentials allows us to easily define them outside the interaction region of the physical Hamiltonian, and is therefore ideal for the computation of molecular resonances.

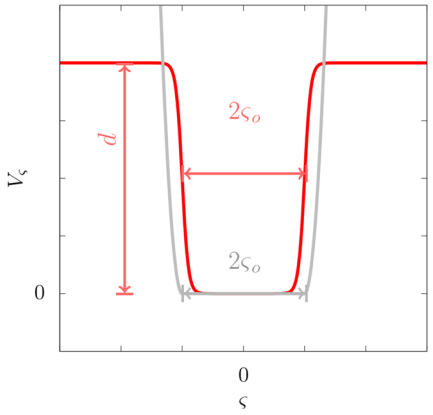

Figure 2. CR-A (gray) and the CR-B (red) potentials.

The modified Hamiltonian, H^m, is first represented in a chosen basis set. Its discrete eigen solutions can be easily computed using conventional *ab initio* quantum chemical methods. Here, Ψ_Q^m is obtained as a bound state localized in the interaction region of H, and the eigen spectrum is naturally partitioned as Q and $\{1 - Q\}$ *spaces*.[43]

$$\mathbf{H}^m = \left(\begin{array}{c|ccccc} E_Q^m & 0 & 0 & \cdots & 0 \\ \hline 0 & E_{\{1-Q\}_1}^m & 0 & \cdots & 0 \\ 0 & 0 & E_{\{1-Q\}_2}^m & \cdots & 0 \\ \vdots & \vdots & \vdots & \ddots & \vdots \\ 0 & 0 & 0 & \cdots & E_{\{1-Q\}_n}^m \end{array}\right) \tag{20}$$

Step 2: *Construction of the $\mathcal{P}$ space.*

Removing the confinement potential, which results in the dissemination of the $\{1 - Q\}$ *space* eigenfunctions, yields the $\mathcal{P}$ *space*. In practice, the physical Hamiltonian H (without the confinement) is first represented in the $\{1 - Q\}$ *space*, and the resulting matrix $\{\ \mathbf{1} - \mathbf{Q}\ \}\mathbf{H}\{\ \mathbf{1} - \mathbf{Q}\ \}$ is a dense matrix. Its diagonal representation gives us the $\mathbf{U}$ matrix and, thus, the $\mathcal{P}$ space.

$$\mathbf{U}^{\dagger}(\{1 - \mathbf{Q}\}\mathbf{H}\{1 - \mathbf{Q}\})\mathbf{U} = \mathbf{E_P} = \begin{pmatrix} E_{P_1} & 0 & \cdots & 0 \\ 0 & E_{P_2} & \cdots & 0 \\ \vdots & \vdots & \ddots & \vdots \\ 0 & 0 & \cdots & E_{P_n} \end{pmatrix} \tag{21}$$

Step 3: *Construction of $\mathcal{QP}$-partitioned H.*

The matrix representation of physical Hamiltonian in the $\{Q \oplus \mathcal{P}\}$ *space* forms the partitioned matrix

$$\mathbf{H} = \left(\begin{array}{c|cccc} E_Q & H_{QP_1} & H_{QP_2} & \cdots & H_{QP_n} \\ \hline H_{P_1Q} & E_{P_1} & 0 & \cdots & 0 \\ H_{P_2Q} & 0 & E_{P_2} & \cdots & 0 \\ \vdots & \vdots & \vdots & \ddots & 0 \\ H_{P_nQ} & 0 & 0 & \cdots & E_{P_n} \end{array}\right) \tag{22}$$

We refer this approach of obtaining *inner−outer* based $\mathcal{QP}$ -partitioned H using a real-valued continuum-remover potential as continuum-remover Feshbach Projection Operator (CR-FPO) formalism. The following are the six major practical advantages of the CR-FPO formalism:

1. A unique $\mathcal{QP}$ partitioning.
   In numerical calculation $\Delta = 0$ corresponds to a unique $\mathcal{QP}$ partitioning.

https://doi.org/10.1021/acs.jctc.1c01096
J. Chem. Theory Comput. 2022, 18, 2863−2874

$$\Delta = \sum_i \frac{H_{QP_i} H_{P_iQ}}{E_{res} - E_{P_i}} \approxeq \sum_i \frac{H_{QP_i} H_{P_iQ}}{E_Q - E_{P_i}} = 0 \tag{23}$$

Since, $E_{res} = E_Q$, the CR method can also be considered as a L^2 stabilization method.

2. Siegert width.

When $\Delta = 0$, the relaxation of Ψ_Q to the $\mathcal{P}$ space results in the so-called L^2 stabilized total wave function Ψ. Therefore, the relaxation of Ψ_Q to Ψ should carry the information on Siegert width.

For $\Delta = 0$ cases, our numerical calculations on a model potential and the doubly excited state of helium, where the exact results are known, show that the quantity that accounts for the dissipation of Ψ_Q^m to the $\mathcal{P}$ *space*

$$\Gamma \approx 2\pi \sum_i |H_{QP_i}|^2 \tag{24}$$

is nothing but the Siegert decay width. This can be further understood as follows. As shown in eq 21, the $\mathcal{P}$ space is obtained from the $\{1 - Q\}$ *space* by removing the CR potential and by doing a unitary transformation.

$$|\psi_\mu\rangle = \sum_i |\psi_i^m\rangle \mathbf{U}_{i\mu} \quad \{\psi\} \in \mathcal{P} \quad \{\psi^m\} \in \{1 - Q\} \tag{25}$$

Since the spatial confinement enforced by the CR potential is removed, the unitary transformation allows the relaxation of $\{1 - Q\}$ *space* from the interaction region toward the asymptote setup by the finite basis set. Therefore, when Ψ_Q^m, which is localized inside the interaction region and having energy $E_Q = E_{res}$, is coupled to the newly constructed $\mathcal{P}$ space through the physical Hamiltonian, a decay equivalent to Siegert decay occurs to the outer region via dissipation through the $\mathcal{P}$ space. See the Supporting Information for an alternate view on the Siegert width occurring due to the unitary transformation.

3. Absence of a uniquely represented $\chi_{E_{res}}$.

As Lippmann and O'Malley pointed out, one of the most important consequences of $\Delta = 0$ is that Ψ_Q and Ψ_P are degenerate and orthogonal.[39] However, since we have chosen the stabilized region of the stabilization plot, a unique representation of $\Psi_P \equiv \chi_{E_{res}}$, similar to that of Ψ_Q^m, is absent in the discrete spectrum. In other words a unique $Q\mathcal{P}$ partitioning (i.e., $\Delta = 0$) and the absence of $\chi_{E_{res}}$—the two characteristics of the stabilized region—are central to the CR-FPO formalism. When $\Delta \neq 0$, the *inner*−*outer* partition is not achieved perfectly and one or many of the discrete functions of $\mathcal{P}$ *space* poorly approximates χ_E. It is worth to note that, although $\Delta = 0$ is central to the CR-FPO formalism, in the cases when $\Delta \neq 0$, one could still use the Stieltjes-moment theory technique or similar methods to extract a continuous approximation for Γ from a discrete representation of the continuum.[36,42] It is important to note that, although a $Q\mathcal{P}$ separability is discussed in the original formulation of the CR potential method[43] and its subsequent applications,[46] unlike the CR-FPO formalism here, the attained $Q\mathcal{P}$ separability was not based on an explicit *inner*−*outer* based partition, and moreover, the $\Delta = 0$ condition was not imposed. Therefore, in those cases a continuous approximation for Γ is necessary to extract the Siegert width.

4. Since the method utilizes L^2 basis functions exclusively, its implementation requires only existing atomic and molecular quantum chemistry codes.

5. Although the asymptotic condition of $\chi_{E_{res}}$ as appears in eq 11 is a strict condition, by noting the fact that the integrals contributing to Γ and Δ become nonzero only inside the *inner* region where Ψ_Q^m is non-negligible, the *inner*−*outer* QP-partitioning allows us to overlook the asymptotic condition of $\chi_{E_{res}}$ as given in eq 11. Moreover, as discussed above, when $\Delta = 0$, a unique representation of $\chi_{E_{res}}$ itself is absent.

6. Because of the *inner*−*outer* QP partitioning, the numerically accurate energy position and width can be obtained using a finite L^2 basis set that satisfies the completeness inside the interaction volume. Additionally, the real-valued continuum-remover potential helps to achieve a faster convergence of the *ab initio* calculation of Ψ_Q^m by removing the basis set artifices such as the oscillatory divergence[47] and nonphysical stabilizations.[48]

3. NUMERICAL TESTS

In this section we describe a practical implementation of the CR-FPO formalism within the framework of bound state methods and we present numerical results. To demonstrate that the proposed CR-FPO formalism works, and in order to test its numerical accuracy, the new formalism is first applied to a one-dimensional model Hamiltonian

$$\hat{H} = -\frac{1}{2}\frac{d}{dx^2} + (0.5x^2 - 0.8)\, e^{-0.1x^2} + 0.8 \tag{26}$$

for which the exact results for the resonance position and the width are known.[49] Therefore, it has been widely used as a test case for new computational procedures.[49−51] Further, the new procedure is applied to the calculation of the lowest doubly excited ^1S resonance state of helium and the lowest doubly excited $^1\Sigma_g^+$ resonance state of molecular hydrogen. As being the most fundamental systems that autoionize and are best suited as benchmark cases for theoretical treatments of autoionization phenomena, these autoionization states have received a great deal of attention.[40,48,52−55]

3.1. Computational Details. For the three test cases, the respective Hamiltonians are represented in a Gaussian basis set, and an exact diagonalization procedure (full CI method) is followed. The implementation of the CR-FPO approach for the exact diagonalization procedure is simple and straightforward. We begin our formal treatment of the CR-FPO formalism by constructing a finite dimensional matrix representation of the modified electronic Hamiltonian $\hat{H}^m = \hat{H}(x) + \hat{W}(x)$ in a basis set. The Q *space* and the $\{1 - Q\}$ *space* are obtained as eigenfunctions of H^m, where the Q *space* is identified as eigenfunctions of H^m which are "stable" against the variation of the continuum-remover potential strength λ or depth d of the confinement potential. The $\mathcal{P}$ *space* is constructed as explained in Step 2 of section 1.

A flow diagram depicting the computational procedure is shown in Figure 3. The width and the energy positions are computed for $\Delta = 0$, which is achieved by varying the strength λ (or depth d) of the continuum-remover potential. In cases when Δ is not converging to zero, scaling the exponents of the diffused

https://doi.org/10.1021/acs.jctc.1c01096
J. Chem. Theory Comput. 2022, 18, 2863−2874

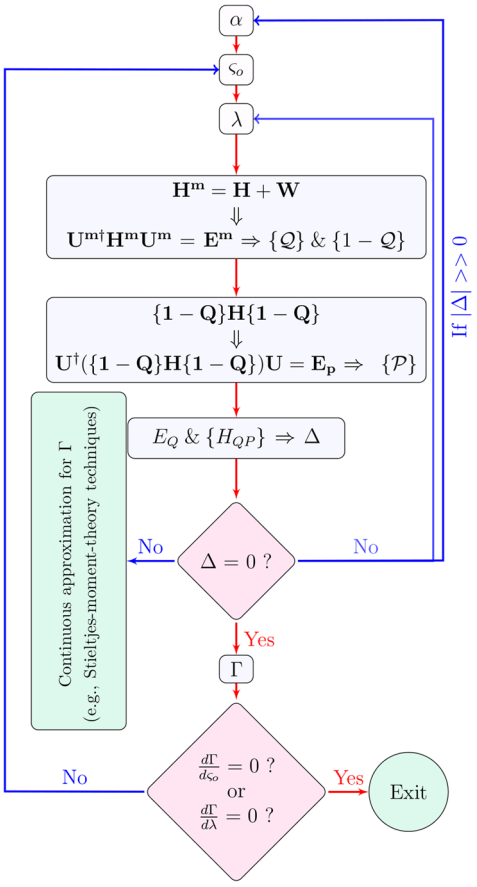

Figure 3. A flow diagram for the computation of resonance energy position and width.

basis functions and choosing a different basis set are practical alternatives, and α in the flow diagram represents this step. Once the $\Delta = 0$ condition is achieved, the energy position becomes the expectation value of the physical Hamiltonian for the $\mathcal{Q}$ *space* wave function. Therefore, the energy position is not directly dependent on the continuum-remover potential. The energy position becomes independent of the potential if the $\mathcal{Q}$ *space* wave function is completely localized inside the interaction region, that is, when the continuum-remover potential is defined outside the interaction. For a complete basis set, once the continuum-remover potential is defined outside the interaction region, the width will converge with respect to the optimal turn-on points (ς_0) of the potential, that is, $\frac{d\Gamma}{d\varsigma_0} = 0$. However, since the $\mathcal{P}$ space wave functions span both the interaction and the noninteraction regions, for a finite basis set, one needs to find the optimal ς_0 for computing the width. For a finite basis set, a cusp condition in the Γ versus ς_0 plot, where $\frac{d\Gamma}{d\varsigma_0} = 0$, identifies the optimal width. Alternatively, a cusp condition corresponding to the λ (or depth d) of the continuum-remover potential can also be used, that is, $\frac{d\Gamma}{d\lambda} = 0$, to get the optimal turn-on points.

3.2. Results. *3.2.1. One-Dimensional Model Hamiltonian.* The one-dimensional model Hamiltonian (eq 26) serves as an ideal test case to demonstrate the basic ideas of the CR-FPO formalism. An even-tempered one-electron Gaussian basis set

$$\{\phi_i = e^{-1000(0.701703846^{i-1})x^2}\}_{i=1,\text{to}\,40} \quad (27)$$

is used for representing the model Hamiltonian.

Since the $\mathcal{Q}$ *space* wave function is an optimal projection of the total wave function inside the model potential well, the $\Delta = 0$ condition is also easily achieved by varying the parameters used in the continuum-remover potential (see Figure 4). Our

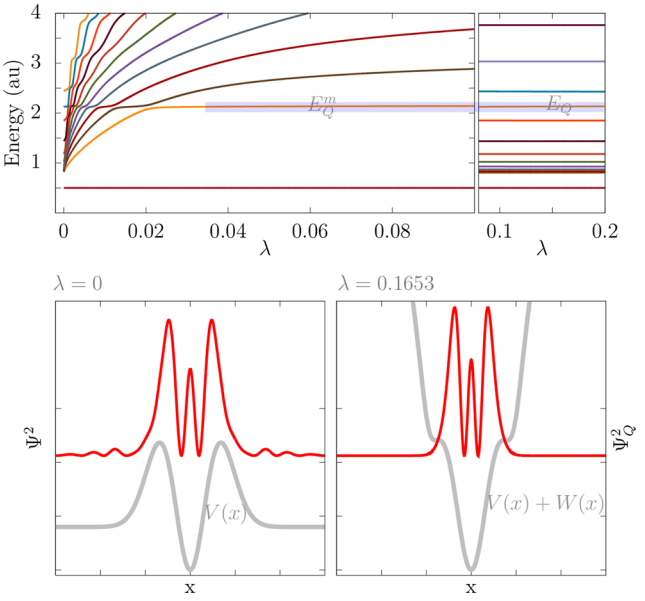

Figure 4. Discrete energy of the modified Hamiltonian in the $\{1 - \mathcal{Q}\}$ *space* (top-left) and the energy of the physical Hamiltonian in the $\mathcal{P}$ *space* (top-right) as a function of the strength of the continuum-remover potential (λ) are shown. The energy position of the $\mathcal{Q}$ *space* wave function is highlighted using a blue color background line. The lower panels show the total wave function obtained from the stabilization method and its $\mathcal{Q}$ *space* projection obtained using the continuum-remover potential.

numerical results are summarized in Table 1, where our results are also compared with the result obtained using continuum remover complex absorbing potential[48] (see Supporting Information for more details) and also with the exact results. The very good agreement between our numerical results and the exact results gives us a great confidence in the CR-FPO approach to expand the formalism for atomic and molecular systems.

3.2.2. The Lowest Doubly Excited States of Helium and Molecular Hydrogen. As discussed in the previous section, because of the explicit use of *inner*−*outer* partitioning, the CR-FPO formalism relies only on the ability of the basis set to span the inner region, that is, the interaction region. Therefore, even a compact Gaussian basis set, which is locally complete inside the interaction region, is expected to produce accurate results. To test the performance of CR-FPO formalism over different choices of basis sets, we have performed two sets of calculations for helium: one with a standard Gaussian basis set saturated with even-tempered primitive Gaussians and the second with a compact Gaussian basis set which is augmented with only a few number of even-tempered primitive Gaussians. A saturated basis set is used for computing the lowest $^1\Sigma_g^+$ resonance state of H_2 molecule. The exponents of these basis sets are given in the Supporting Information.

Numerical results for the ^1S resonance state of the helium atom obtained using the CR-FPO formalism and other methods are summarized in Tables 2 and 3. The results obtained from CR-FPO formalism and various theoretical methods for the $^1\Sigma_g^+$

https://doi.org/10.1021/acs.jctc.1c01096
J. Chem. Theory Comput. 2022, 18, 2863−2874

Table 1. Energy and Half-Width as a Function of the Turn-on Point x_o of the Confinement Potentials[a]

CR-A (eq 18)				CR-B (eq 19)			
x_o (au)	λ	E_{res} (au)	$\Gamma/2$ (au)	x_o (au)	d	E_{res} (au)	$\Gamma/2$ (au)
5.00	0.08567	2.127120	0.017586	5.75	5.61700	2.127120	0.0170080
5.25	0.11648	2.127120	0.017352	6.00	8.57700	2.127120	0.016840
5.50	0.16530	***2.127120***	***0.017301***	6.25	13.42500	***2.127120***	***0.016784***
5.75	0.24375	2.127120	0.017384	6.50	21.38500	2.127120	0.016797
6.00	0.37090	2.127120	0.017556	6.75	34.47000	2.127120	0.016853
continuum-remover CAP (same basis set; x_o = 5.50 au)						2.126355	0.0149037
exact (Ref 49)						2.127197	0.015447

[a]The optimized values are in ***bold-italic*** font.

Table 2. Energy and Width of the Lowest $^1S(2s^2)$ Autoionizing Resonance State of Helium Using a Saturated Basis Set[a,b]

CR-A (eq 17)				CR-B (eq 19)			
ς_o (au)	λ	E_{res} (au)	Γ(au)	ς_o (au)	d	E_{res} (au)	Γ(au)
9	1.92	−0.777144	0.005137	10	9.4	−0.777144	0.005983
10	5.01	***−0.777144***	***0.005127***	11	23.9	−0.777144	0.005157
11	13.6	−0.777144	0.005215	12	65.2	***−0.777144***	***0.004960***
12	38.8	−0.777144	0.005335	13	185	−0.777144	0.004999
complex scaling (same basis set)						−0.777781	0.0041282
RFCAP (ref 54)						−0.77529	0.00494
accurate (ref 40)						-0.7788133	0.0045937

[a]$x_o = y_0 = z_o = \varsigma_o$. [b]The optimized resonance parameters are in ***bold-italic*** font.

Table 3. Energy and Width of Lowest $^1S(2s^2)$ Autoionizing Resonance State of Helium Using a Compact Basis Set[a,b]

CR-A (eq 17)				CR-B (eq 19)			
ς_o (au)	λ	E_{res} (au)	Γ (au)	ς_o (au)	d	E_{res} (au)	Γ (au)
8	3.2	−0.776092	0.005838	9	7.49	−0.776092	0.010117
9	18.38	***−0.776092***	***0.005685***	10	23.4	−0.776092	0.006808
10	120	−0.776092	0.005956	11	97.5	−0.776092	0.005684
11	860	−0.776092	0.006279	12	482	***−0.776092***	***0.005540***
complex scaling (same basis set)						−0.775737	0.00222
accurate (ref 40)						−0.778813	0.0045937

[a]$x_o = y_0 = z_0 = \varsigma_o$. [b]The optimized resonance parameters are in ***bold-italic*** font.

Table 4. Energy Position and Width of Lowest $^1\Sigma_g^+$ Autoionizing Resonance State of H_2[a,b]

CR-A (eq 17)				CR-B (eq 19)			
ςo (au)	λ	E_{res} (au)	Γ (au)	ςo (au)	d	E_{res} (au)	Γ (au)
4	0.098	0. 479681	0.021367	7	2.93	0. 479681	0.020128
5	0.37	***0. 479681***	***0.019981***	8	12	***0. 479681***	***0.019408***
6	1.75	0. 479681	0.020567	9	54	0. 479681	0.020161
7	8.9	0. 479681	0.023919	10	280	0. 479681	0.021504
complex back-rotation method (ref 52)						0.4618	0.0197
reflection-free CAP (ref 53)						0.4615	0.0227
continuum remover CAP (ref 48)						0.4648	0.0178

[a]$x_o = y_0 = z_0 - \frac{R}{2} = \varsigma_o$; R = 1.4 au. [b]The optimized resonance parameters are in ***bold-italic*** font.

resonance state of H_2 are listed in Table 4. Our results for positions and widths are in good agreement with the accurate results reported in the literature.

As expected, the CR-FPO formalism produces numerically reliable results using both saturated and compact basis sets. Most interestingly, for these finite Gaussian basis sets, the CR-FPO formalism performed even better than the complex scaling method. The methods such as complex scaling depend on asymptotic quality of the basis set, whereas the *inner−outer* partitioning allows the CR-FPO formalism to obtain the resonance parameters using a basis set that satisfies the completeness inside the inner region. This fact is also expected to give greater computational advantages when CR-FPO formalism is used in conjunction with the effective Hamiltonian methods.[56] Instead of the brute-force exact diagonalization procedure, using a correlation operator, also known as the wave operator, the effective Hamiltonian approaches solve the eigenvalue problem in a smaller dimensional function space, and obtain the exact energies as the eigenvalues.[56] To check the performance of the CR-FPO formalism within the effective Hamiltonian approach, we have done a new set of calculations in which we have used the discrete eigenstates of the physical

https://doi.org/10.1021/acs.jctc.1c01096
J. Chem. Theory Comput. 2022, 18, 2863−2874

Table 5. Effect of the Size of Effective Hamiltonian Matrix on the ^1S Resonance State of Helium[a]

	CR-A (eq 17) (ς_o = 10 au)			CR-B (eq 19) (ς_o = 12 au)			complex scaling	
$\mathbf{H}_{\text{eff}}$ size	λ	E_{res} (au)	Γ (au)	d	E_{res} (au)	Γ (au)	E_{res} (au)	Γ (au)
100	2.20	−0.777144	0.009814	52.75	−0.777144	0.004917		
250	3.72	−0.777144	0.005395	54.67	−0.777144	0.004884		
500	4.95	−0.777144	0.005110	64.80	−0.777144	0.004923	−0.77629	0.01595
FCI	5.01	−0.777144	0.005127	65.20	−0.777144	0.004960	−0.77778	0.00413

[a] $x_o = y_0 = z_0 = \varsigma_o$.

Table 6. Effect of the Size of Effective Hamiltonian Matrix on the $^1\Sigma_g^+$ Resonance State of Molecular Hydrogen[a]

	CR-A (eq 17) (ς_o = 5 au)			CR-B (eq 19) (ς_o = 8 au)		
$\mathbf{H}_{\text{eff}}$ size	λ	E_{res} (au)	Γ (au)	d	E_{res} (au)	Γ (au)
25	1.35	−0.090289	0.015080	17.55	−0.090289	0.015695
50	0.414	−0.090289	0.015465	13.4	−0.090289	0.015498
100	0.403	−0.090289	0.015844	13.16	−0.090289	0.015897
250	0.373	−0.090289	0.017807	12.05	−0.090289	0.017530
500	0.371	−0.090289	0.018908	12.00	−0.090289	0.018447
FCI	0.370	−0.090289	0.019981	12.00	−0.090289	0.019408

[a] $x_o = y_0 = z_0 - \frac{R}{2} = \varsigma_o$; R = 1.4 au.

Hamiltonian diagonalized in the saturated Gaussian basis as the electronic basis, that is, the full CI states are used as the basis set for the CR-FPO formalism. The Hamiltonian represented in a subset of full-CI states can be considered as an effective Hamiltonian matrix, $\mathbf{H}_{\text{eff}}$. Our results are summarized in Tables 5 and 6, where the size of the effective Hamiltonian is varied. The CR-FPO method produces very accurate results even when the size of the effective Hamiltonian is considerably small. To further understand the computational benefit of the CR-FPO over other methods, the results obtained from the complex scaled effective Hamiltonian are also given in Table 5. Complex scaling does not even produce complex stabilized points when the size of the effective Hamiltonian matrix is small. It is also worth noting that, throughout our numerical tests, the CR-B variant, where the autoionization threshold is shifted above the resonance states, of the CR potential is more consistent and accurate.

Although the resonance states we have computed for the model potential and the two electron systems are the lowest resonance states, they are not the lowest eigenstates of the respective symmetry block of the Hamiltonian matrix. Therefore, computationally the CR-FPO method should also work for other higher resonances. To verify the performance of the CR-FPO method for higher resonance states, we computed two resonances of the He atom belonging to the same symmetric block of the Hamiltonian. The results are presented in Table 7. These results clearly demonstrate that the CR-FPO method can be used for computing higher resonances.

Table 7. Energy and Width of the First Three ^1S Autoionizing Resonance State of Helium Using a Saturated Basis Set[a]

CR-B (eq 19) (ς_o = 12 au)			ref 57	
d	E_{res} (au)	Γ (au)	E_{res} (au)	Γ (au)
65.2	−0.777144	0.004960	−0.777867	0.00454
31.5	−0.616867	0.000173	−0.621927	0.00021
40.4	−0.589485	0.00143	−0.589894	0.00136

[a] $x_o = y_0 = z_0 = \varsigma_o$

4. IMPLEMENTATION OF CR-FPO FORMALISM IN THE MULTIREFERENCE CONFIGURATION INTERACTION METHOD

In our implementation of CR-FPO formalism within the multireference configuration interaction (MRCI) method, we employ the effective Hamiltonian approach as discussed in section 2, that is, we use the state vectors as the initial basis set to set up the CR-FPO formalism. The benefit of an effective Hamiltonian approach is that it allows us to work in a reduced dimensional space, which leads to saving on computational time, while still obtaining accurate results. For a given one-particle atom-center basis set, the state vectors that span the domain of the physical effective Hamiltonian are obtained from a standard MRCI calculation. A suitable one-particle basis for computing the state vectors is chosen with the help of a stabilization method, which is done as follows:

- A series of scaled basis sets ranging from most-diffuse to most-contracted are generated by augmenting a standard parent basis set with an additional set of even-tempered Gaussians and by scaling the exponent of the most diffuse functions with a finite value.
- In the next step, we generate the stabilization curve for a given system by computing and plotting the eigenvalues at the MRCI level for the scaled basis sets. The stabilized region is identified for the resonant state, and the corresponding state-vectors are chosen for subsequent CR-FPO calculations. One of the reasons for choosing a basis set from the stabilization procedure is that the energy position obtained from the stabilization method can be used as a benchmark result to test the numerical accuracy of the CR-FPO-MRCI result.
- The final CR-FPO approach is set up in the state vector basis, and the procedure summarized in Figure 3 is followed to estimate the optimum resonance parameters.

4.1. Computational Details. We have used the MRCI method as implemented in the COLUMBUS quantum chemistry code.[58−61] The V_{CR} used in the current work is an infinite well potential of the form given in eq 16, and the V_{CR} integrals are imported from the OpenCAP software.[62] We have

https://doi.org/10.1021/acs.jctc.1c01096
J. Chem. Theory Comput. 2022, 18, 2863−2874

used Dunning's augmented correlation-consistent triple-valence zeta basis (aug-cc-pVTZ) as the one-electron parent basis, which is further augmented with a set of evenly tempered [2s2p2d] functions. The even-tempered Gaussians are generated according to the expression $x_i = xf^{i-1}$, where x is the exponent of the most diffuse s, p, or d function in the parent basis, x_i is the new exponent of the even-tempered Gaussian and f is kept at 0.50. The N−N bond distance is set at 2.077 au.

All the calculations for generating the stabilization plots for N_2^- are performed at the MRCI with single excitations (MRCIS) level using an active space of 5 electrons in 8 orbitals, (5,8). The active space includes the valence π and π^* orbitals and a set of two degenerate diffuse orbitals of symmetry corresponding to that of the resonance state. Two sets of MRCIS calculations are done using orbitals from a CASSCF solution with state-averaging over 10 (SA-10) and 15 (SA-15) states, respectively. The resonance position is reported as the difference between the energies of the N + 1-electron resonance wave function and N-electron target energy, that is, $E_{res}^{position} = E_{res}^{N+1} - E_{target}^{N}$. The energy of the neutral target state is computed at the MRCI level by employing the same orbitals used to describe the negative ion resonance state and a (4,8) active space.

4.2. Results-$^2\Pi_g$ Resonance in N_2^-. The $^2\Pi_g$ shape resonance of N_2^- is one of the most well studied systems using a variety of theoretical methods.[63−69] The electron attachment to the valence π^* orbitals leads to the formation of a $^2\Pi_g$ shape resonance. In this work, we report the results for the $\alpha = 1.4$ basis set for which the resonance state becomes stable and is represented by a single discrete state (see Figure 5). For a given choice of turn-on points of the continuum-remover potential, the width and the energy positions are computed for $\Delta = 0$, which is achieved by varying the strength λ of the confinement potential. Our numerical results obtained for various turn-on points of the continuum-remover potential are tabulated in Table 8. Further, optimum turn-on points (x_0,y_0 and z_0) of the V_{CR} are identified by the corresponding cusp in the values for resonance widths. See section 3.1 for a detailed discussion of computing the energy position and width by varying the basis set parameters and continuum-remover potential parameters. The computed values for position and width at the optimized turn-on points are 2.78 and 0.14 eV, respectively. Most importantly, for the chosen basis set (α = 1.4) and the level of electron correlation used (i.e., MRCIS), the energy position obtained using CR-FPO formalism and the stabilization formalism are the same.

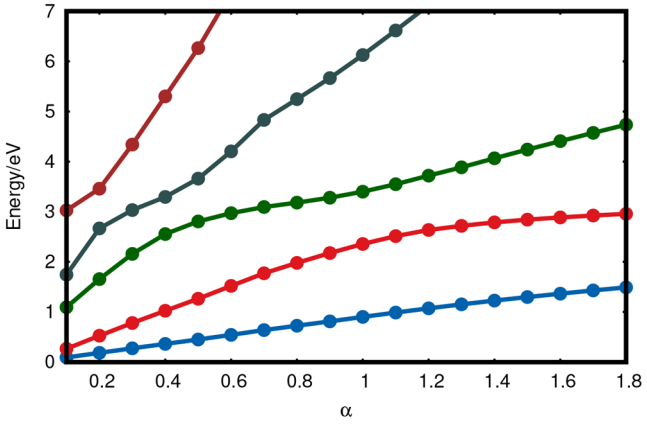

Figure 5. Stabilization curve for the $^2\Pi_g$ resonance in N_2^- obtained at the SA10-MRCIS(5,8)/aug-cc-pVTZ+[2s2p2d] level of theory.

For a meaningful comparison with the results obtained from other theoretical methods, it is worth noting that the energy position and the width in the case of the CR-FPO formalism depends only on the accuracy of the underlying *ab initio* quantum chemical method and corresponding treatment of electronic correlation. In the standard *ab initio* quantum chemical formalism, the energy position can either be computed *directly*, that is, the energy position is directly obtained as an eigenvalue of a modified energy operator, or by subtracting the target state energy from the resonance state energy. Because of the consistent treatment of electron correlation for both the neutral target and the final resonance state, the methods that compute the energy position *directly* and include higher levels of excitation correlation are more reliable compared to any of the *indirect* methods unless the *indirect* method also includes higher levels of excitation correlation to overcome the inconsistent treatment of electron correlation. To make the comparison more meaningful, the literature reported values of resonance parameters for the $^2\Pi_g$ resonance from the *direct difference* methods, and *indirect* methods are tabulated in Table 9. Considering the fact that our MRCI is not a direct energy difference method, and only *singles* levels of excitation correlation are included at the MRCI level, our results are in agreement with the highly correlated *direct* methods within the limits of the level of electron correlation used. Furthermore, on the basis of the numbers reported in Table 8, the results also converge faster with the size of the effective Hamiltonian. The underestimation of width could be attributed to several factors such as inclusion of only singles level excitation, deficiencies in active space, and small size of the effective Hamiltonian. To test our hypothesis about the importance of double excitations, we have performed preliminary CR-FPO/MRCISD calculations using an MRCI expansion with single and double excitations.

Table 8. Energy Positions and Widths for the $^2\Pi_g$ Resonance in N_2^- at MRCIS(5,8)/aug-cc-pVTZ+[2s2p2d] Level of Theory[a]

	SA-10			SA-15		
box size (au)	E_{res} (eV)	Γ (eV)	λ_{opt} (au)	E_{res} (eV)	Γ (eV)	λ_{opt} (au)
$x_0 = y_0 = 2.76$, $z_0 = 4.88$	2.79	0.0945	0.00677	2.78	0.0936	0.00674
$x_0 = y_0 = 3.76$, $z_0 = 5.88$	2.79	0.102	0.0139	2.78	0.102	0.0138
$x_0 = y_0 = 4.76$, $z_0 = 6.88$	2.79	0.115	0.0325	2.78	0.115	0.0322
$x_0 = y_0 = 5.76$, $z_0 = 7.88$	2.79	0.129	0.0881	2.78	0.128	0.0867
$x_0 = y_0 = 6.76$, $z_0 = 8.88$	2.79	0.141	0.281	2.78	0.139	0.274
$x_0 = y_0 = 7.76$, $z_0 = 9.88$	***2.79***	***0.147***	***1.07***	***2.78***	***0.143***	***1.04***
$x_0 = y_0 = 8.76$, $z_0 = 10.88$	2.79	0.141	4.92	2.78	0.132	4.58

[a]The optimized resonance parameters are in ***bold-italic*** font.

https://doi.org/10.1021/acs.jctc.1c01096
J. Chem. Theory Comput. 2022, 18, 2863−2874

Table 9. Energy Position ($E_{res}^{position} = E_{res}^{N+1} - E_{target}^{N}$) and Width of the $^2\Pi_g$ Resonance in N_2^- from Selected Previous Works

selected works		method	$E_{res}^{position}$ (eV)	Γ (eV)
Direct computation of $E_{res}^{position}$	Meyer[64]	Optical potential/ ADC(3)	2.534	0.536
	Sajeev *et al.*[65]	CAP/FSMRCC	2.52	0.39
	Sven *et al.*[70]	CAP/EP	2.58	0.55
	Zuev *et al.*[66]	CAP/EOM-EA-CCSD	2.571	0.255
	Ghosh *et al.*[71]	CAP/EOM-EA-CCSD	2.07	0.420
	Thodika et al.[72]	OSM/EOM-EA-CCSD	2.525	0.493
	Das et al.[67]	CAP/EP-MCSCF	3.117	0.313
$E_{res}^{position}$ using indirect methods	Hazi et al.[63]	Stieltjes-moment theory/ Static and exchange	4.13	1.14
	Hazi et al.[63]	Stieltjes-moment theory/CIS	2.23	0.40
	Chao et al.[73]	Stabilization/ MRCI	2.34	0.51
	Sommerfeld et al.[68]	CAP/MRCISD	2.97	0.65
	this work	Stabilization/ MRCIS	2.78	
	this work	CR-FPO/ MRCIS	2.78	0.143
	this work	CR-FPO/ MRCISD	2.87	0.636

These results show a significant improvement in the computed width (see Table 10). These calculations are done using the orbitals from a CASSCF method with state averaged over 10 states, and with the same active space as that of the MRCIS method. Most importantly, the inclusion of the double excitation increases the interaction volume compared to the MRCI method. In other words, the artificial shrinking of the interaction region due to the poor description of the $\mathcal{Q}$ *space* and $\mathcal{P}$ *space* wave functions is also one of the major reasons for the underestimation of width in the MRCIS method. We would also like to emphasize here that the results presented in Table 10 are preliminary results, and further benchmarking of the CR-FPO/MRCISD method will be performed in a future publication. A more rigorous study on the dependence of resonance parameters on active space, basis set, effective Hamiltonian size, and electronic structure methods is required for an appropriate comparison of our results with predictions in the literature. Therefore, it is worth emphasizing that the primary objective of implementing the CR-FPO within the MRCI method at the *singles* levels of excitation correlation is solely to demonstrate the feasibility of the new formalism to use in conjunction with the standard *ab initio* codes.

Table 10. Energy Positions and Widths for the $^2\Pi_g$ Resonance in N_2^- at MRCISD Level of Theory[a]

box size (au)	E_{res} (eV)	Γ (eV)	λ_{opt} (au)
$x_0 = y_0 = 6.76, z_0 = 8.88$	2.87	0.310	0.234
$x_0 = y_0 = 7.76, z_0 = 9.88$	2.87	0.329	0.515
$x_0 = y_0 = 8.76, z_0 = 10.88$	2.87	0.359	1.23
$x_0 = y_0 = 9.76, z_0 = 11.88$	2.87	0.411	3.12
$x_0 = y_0 = 10.76, z_0 = 12.88$	2.87	0.507	7.79
$x_0 = y_0 = 11.76, z_0 = 13.88$	2.87	0.611	18.4
$x_0 = y_0 = 12.26, z_0 = 14.38$	***2.87***	***0.636***	29.0
$x_0 = y_0 = 12.76, z_0 = 14.88$	2.87	0.624	47.9
$x_0 = y_0 = 13.26, z_0 = 15.38$	2.87	0.590	83.5
$x_0 = y_0 = 13.76, z_0 = 15.88$	2.87	0.548	151

[a]The optimized resonance parameters are in ***bold-italic*** font.

As we have numerically demonstrated in the case of the Feshbach resonances of He and H_2, which are computed at the full-CI level, a high numerical accuracy in the $E_{res}^{position}$ and width can also be achieved by including higher levels of excitation correlation at the MRCI level.

5. CONCLUSIONS

By combining the Feshbach projection operator formalism and the real-valued continuum-remover potential, a novel technique is developed for computing the resonance energy and the width. Unlike the conventional FPO partitioning of total wave function into its resonant $\mathcal{Q}$ and nonresonant $\mathcal{P}$ components, we partition the total function into *inner* interaction region and *outer* noninteraction region components. The real-valued continuum-remover potential method helps us to project out a unique interaction-region component of the total wave function—for which the level shift is zero—as the $\mathcal{Q}$ *space* wave function without sacrificing the computational simplicity inherent in the quantum chemical electronic structure codes. This unique projection makes the direct computation of Siegert width possible. The far superior performance of CR-FPO formalism over other methods with compact Gaussian basis sets, which is due to the *inner*−*outer* based $\mathcal{QP}$ partitioning, is a major breakthrough. The fact that a few $\mathcal{P}$ *space* states are sufficient enough to introduce the relaxation of the $\mathcal{Q}$ *space* wave function to the outer noninteraction region makes the CR-FPO formalism one of the most desirable methods to employ within the framework of bound state quantum chemical codes for the computation of resonance energy and Siegert width.

■ ASSOCIATED CONTENT

Supporting Information

The Supporting Information is available free of charge at https://pubs.acs.org/doi/10.1021/acs.jctc.1c01096.

> The asymptotic electron density change due to $1 - \mathcal{Q}$ *space* to $\mathcal{P}$ *space* transformation, resonance state calculation using the continuum-remover complex absorbing potential and the basis set details (PDF)

■ AUTHOR INFORMATION

Corresponding Author

Y. Sajeev − *Theoretical Chemistry Section, Bhabha Atomic Research Centre, Mumbai 400085, India;* orcid.org/0000-0002-2250-5101; Email: sajeevy@barc.gov.in

Authors

Mushir Thodika − *Department of Chemistry, Temple University, Philadelphia, Pennsylvania 19122, United States;* orcid.org/0000-0002-6837-9710

Spiridoula Matsika − *Department of Chemistry, Temple University, Philadelphia, Pennsylvania 19122, United States;* orcid.org/0000-0003-2773-3979

Complete contact information is available at: https://pubs.acs.org/10.1021/acs.jctc.1c01096

https://doi.org/10.1021/acs.jctc.1c01096
J. Chem. Theory Comput. 2022, 18, 2863−2874

Notes

The authors declare no competing financial interest.

■ ACKNOWLEDGMENTS

M.T. and S.M. acknowledge support by the National Science Foundation (NSF, Grant No. CHE-1800171).

■ REFERENCES

(1) Boudaïffa, B.; Cloutier, P.; Hunting, D.; Huels, M. A.; Sanche, L. Resonant Formation of DNA Strand Breaks by Low-Energy (3 to 20 eV) Electrons. *Science* **2000**, *287*, 1658−1660.
(2) Krishnakumar, E. Electron controlled chemistry. *J. Phys.: Conference Series* **2009**, *185*, No. 012022.
(3) Stipe, B.; Rezaei, M.; Ho, W.; Gao, S.; Persson, M.; Lundqvist, B. Single-molecule dissociation by tunneling electrons. *Phys. Rev. Lett.* **1997**, *78*, 4410.
(4) Abdoul-Carime, H.; Gohlke, S.; Illenberger, E. Site-Specific Dissociation of DNA Bases by Slow Electrons at Early Stages of Irradiation. *Phys. Rev. Lett.* **2004**, *92*, 168103.
(5) Lim, T.; Polanyi, J. C.; Guo, H.; Ji, W. Surface-mediated chain reaction through dissociative attachment. *Nat. Chem.* **2011**, *3*, 85−89.
(6) Davis, D.; Vysotskiy, V. P.; Sajeev, Y.; Cederbaum, L. S. Electron Impact Catalytic Dissociation: Two-Bond Breaking by a Low-Energy Catalytic Electron. *Angew. Chem., Int. Ed.* **2011**, *50*, 4119−4122.
(7) Davis, D.; Vysotskiy, V. P.; Sajeev, Y.; Cederbaum, L. S. Electron Impact Catalytic Dissociation: Two-Bond Breaking by a Low-Energy Catalytic Electron. *Angew. Chem., Int. Ed.* **2012**, *51*, 8003−8007.
(8) Davis, D.; Kundu, S.; Prabhudesai, V. S.; Sajeev, Y.; Krishnakumar, E. Formation of CO_2 from formic acid through catalytic electron channel. *J. Chem. Phys.* **2018**, *149*, No. 064308.
(9) Davis, D.; Sajeev, Y. Low-energy-electron induced permanently reactive CO_2 molecules. *Phys. Chem. Chem. Phys.* **2014**, *16*, 17408−17411.
(10) Martin, F.; Burrow, P. D.; Cai, Z.; Cloutier, P.; Hunting, D.; Sanche, L. DNA Strand Breaks Induced by 0−4 eV Electrons: The Role of Shape Resonances. *Phys. Rev. Lett.* **2004**, *93*, No. 068101.
(11) Arumainayagam, C. R.; Lee, H.-L.; Nelson, R. B.; Haines, D. R.; Gunawardane, R. P. Low-energy electron-induced reactions in condensed matter. *Surf. Sci. Rep.* **2010**, *65*, 1−44.
(12) Alizadeh, E.; Orlando, T. M.; Sanche, L. Biomolecular damage induced by ionizing radiation: the direct and indirect effects of low-energy electrons on DNA. *Annu. Rev. Phys. Chem.* **2015**, *66*, 379−398.
(13) Davis, D.; Bhushan, K. G.; Sajeev, Y.; Cederbaum, L. S. A Concerted Synchronous [2 + 2] Cycloreversion Repair Catalyzed by Two Electrons. *J. Phys. Chem. Lett.* **2018**, *9*, 6973−6977.
(14) Khorsandgolchin, G.; Sanche, L.; Cloutier, P.; Wagner, J. R. Strand Breaks Induced by Very Low Energy Electrons: Product Analysis and Mechanistic Insight into the Reaction with TpT. *J. Am. Chem. Soc.* **2019**, *141*, 10315−10323.
(15) Simons, J. How Do Low-Energy (0.1−2 eV) Electrons Cause DNA-Strand Breaks? *Acc. Chem. Res.* **2006**, *39*, 772−779.
(16) Dong, Y.; Liao, H.; Gao, Y.; Cloutier, P.; Zheng, Y.; Sanche, L. Early Events in Radiobiology: Isolated and Cluster DNA Damage Induced by Initial Cations and Nonionizing Secondary Electrons. *J. Phys. Chem. Lett.* **2021**, *12*, 717−723.
(17) Arumainayagam, C. R.; Garrod, R. T.; Boyer, M. C.; Hay, A. K.; Bao, S. T.; Campbell, J. S.; Wang, J.; Nowak, C. M.; Arumainayagam, M. R.; Hodge, P. J. Extraterrestrial prebiotic molecules: photochemistry vs. radiation chemistry of interstellar ices. *Chem. Soc. Rev.* **2019**, *48*, 2293−2314.
(18) Millar, T. J.; Walsh, C.; Field, T. A. Negative Ions in Space. *Chem. Rev.* **2017**, *117*, 1765−1795.
(19) Davis, D.; Sajeev, Y. A hitherto unknown stability of DNA basepairs. *Chem. Commun.* **2020**, *56*, 14625−14628.
(20) Moiseyev, N. *Non-Hermitian Quantum Mechanics*; Cambridge University Press, 2011.
(21) Moiseyev, N. Quantum theory of resonances: calculating energies, widths and cross-sections by complex scaling. *Phys. Rep.* **1998**, *302*, 212−293.
(22) Santra, R.; Cederbaum, L. S. Non-Hermitian electronic theory and applications to clusters. *Phys. Rep.* **2002**, *368*, 1−117.
(23) Riss, U. V.; Meyer, H. D. Calculation of resonance energies and widths using the complex absorbing potential method. *J. Phys. B* **1993**, *26*, 4503.
(24) Ehara, M.; Sommerfeld, T. CAP/SAC-CI method for calculating resonance states of metastable anions. *Chem. Phys. Lett.* **2012**, *537*, 107−112.
(25) Holoien, E.; Midtdal, J. New Investigation of the $^1S^e$ Autoionizing States of He and H^-. *J. Chem. Phys.* **1966**, *45*, 2209−2216.
(26) Hazi, A. U.; Taylor, H. S. Stabilization Method of Calculating Resonance Energies: Model Problem. *Phys. Rev. A* **1970**, *1*, 1109−1120.
(27) McCurdy, C.; McNutt, J. On the possibility of analytically continuing stabilization graphs to determine resonance positions and widths accurately. *Chem. Phys. Lett.* **1983**, *94*, 306−310.
(28) Simons, J. Resonance state lifetimes from stabilization graphs. *J. Chem. Phys.* **1981**, *75*, 2465−2467.
(29) Feuerbacher, S.; Sommerfeld, T.; Cederbaum, L. S. Extrapolating bound state data of anions into the metastable domain. *J. Chem. Phys.* **2004**, *121*, 6628−6633.
(30) Sommerfeld, T.; Weber, R. J. Empirical Correlation Methods for Temporary Anions. *J. Phys. Chem. A* **2011**, *115*, 6675−6682.
(31) Thodika, M.; Mackouse, N.; Matsika, S. Description of Two-Particle One-Hole Electronic Resonances Using Orbital Stabilization Methods. *J. Phys. Chem. A* **2020**, *124*, 9011−9020.
(32) Dempwolff, A. L.; Belogolova, A. M.; Sommerfeld, T.; Trofimov, A. B.; Dreuw, A. CAP/EA-ADC method for metastable anions: Computational aspects and application to π^* resonances of norbornadiene and 1,4-cyclohexadiene. *J. Chem. Phys.* **2021**, *155*, No. 054103.
(33) Sommerfeld, T.; Ehara, M. Complex Absorbing Potentials with Voronoi Isosurfaces Wrapping Perfectly around Molecules. *J. Chem. Theory Comput.* **2015**, *11*, 4627−4633.
(34) Feshbach, H. Unified theory of nuclear reactions. *Ann. Phys.* **1958**, *5*, 357−390.
(35) Feshbach, H. A unified theory of nuclear reactions. II. *Ann. of Phys.* **1962**, *19*, 287−313.
(36) Hazi, A. U. A purely L^2 method for calculating resonance widths. *J. Phys. B* **1978**, *11*, L259−L264.
(37) Hickman, A. P.; Isaacson, A. D.; Miller, W. H. Feshbach projection operator calculation of the potential energy surfaces and autoionization lifetimes for $He(2^3S)H$ and $He(2^3S)H_2$. *J. Chem. Phys.* **1977**, *66*, 1483−1491.
(38) O'Malley, T. F. Slow Heavy-Particle Collision Theory Based on a Quasiadiabatic Representation of the Electronic States of Molecules. *Phys. Rev.* **1967**, *162*, 98−104.
(39) Lippmann, B. A.; O'Malley, T. F. Unique Definition of the Quasistationary State for Resonant Processes. *Phys. Rev. A* **1970**, *2*, 2115−2124.
(40) Bhatia, A. K.; Temkin, A. Calculation of autoionization of He and H^- using the projection-operator formalism. *Phys. Rev. A* **1975**, *11*, 2018−2024.
(41) Macías, A.; Martín, F.; Riera, A.; Yáñez, M. Simple discretization method for autoionization widths. II. Atoms. *Phys. Rev. A* **1987**, *36*, 4187−4202.
(42) Reinhardt, W. P. L^2 discretization of atomic and molecular electronic continua: Moment, quadrature and J-matrix techniques. *Comput. Phys. Commun.* **1979**, *17*, 1−21.
(43) Sajeev, Y. Real-valued continuum remover potential: An improved L^2-stabilization method for the chemistry of electronic resonance states. *Chem. Phys. Lett.* **2013**, *587*, 105−112.
(44) Liebman, J. F.; Yeager, D. L.; Simons, J. A simple approach to predicting resonance levels. *Chem. Phys. Lett.* **1977**, *48*, 227−232.
(45) Kaijser, P.; Simons, J. Shift-potential approaches for determining shape resonances in atoms: ^2P Be^- and Mg^-. *Phys. Rev. A* **1980**, *21*, 1093−1099.

https://doi.org/10.1021/acs.jctc.1c01096
J. Chem. Theory Comput. 2022, 18, 2863−2874

(46) Kunitsa, A. A.; Bravaya, K. B. Feshbach projection XMCQDPT2 model for metastable electronic states. , *arXiv* (Physics-Chemical Physics) ver. 1, 1906.11390, Jun 26, 2019. https://arxiv.org/abs/1906.11390, (accessed 2022-02-05).
(47) Peirs, K.; Van Neck, D.; Waroquier, M. Self-consistent solution of Dysons equation up to second order for open-shell atomic systems. *J. Chem. Phys.* **2002**, *117*, 4095−4105.
(48) Sajeev, Y.; Vysotskiy, V.; Cederbaum, L. S.; Moiseyev, N. Continuum remover-complex absorbing potential: Efficient removal of the nonphysical stabilization points. *J. Chem. Phys.* **2009**, *131*, 211102.
(49) Davidson, E. R.; Engdahl, E.; Moiseyev, N. New bounds to resonance eigenvalues. *Phys. Rev. A* **1986**, *33*, 2436−2439.
(50) Lipkin, N.; Moiseyev, N.; Brändas, E. Resonances by the exterior-scaling method within the framework of the finite-basis-set approximation. *Phys. Rev. A* **1989**, *40*, 549−553.
(51) Rom, N.; Moiseyev, N. Absorbing boundary conditions by the partial integration exterior scaling method. *J. Chem. Phys.* **1993**, *99*, 7703−7708.
(52) Balanarayan, P.; Sajeev, Y.; Moiseyev, N. Ab-initio complex molecular potential energy surfaces by the back-rotation transformation method. *Chem. Phys. Lett.* **2012**, *524*, 84−89.
(53) Sajeev, Y.; Moiseyev, N. Reflection-free complex absorbing potential for electronic structure calculations: Feshbach-type autoionization resonances of molecules. *J. Chem. Phys.* **2007**, *127*, No. 034105.
(54) Sajeev, Y.; Sindelka, M.; Moiseyev, N. Reflection-free complex absorbing potential for electronic structure calculations: Feshbach type autoionization resonance of Helium. *Chem. Phys.* **2006**, *329*, 307−312.
(55) Moiseyev, N. Derivations of universal exact complex absorption potentials by the generalized complex coordinate method. *J. Phys. B:* **1998**, *31*, 1431−1441.
(56) Lindgren, I.; Morrison, J. *Atomic Many-Body Theory*; Springer: Berlin, Heidelberg, 2012.
(57) Burgers, A.; Wintgen, D.; Rest, J. M. Highly doubly excited S states of the helium atom. *J. of Phys. B* **1995**, *28*, 3163−3183.
(58) Lischka, H.; Shepard, R.; Pitzer, R. M.; Shavitt, I.; Dallos, M.; Muller, T.; Szalay, P. G.; Seth, M.; Kedziora, G. S.; Yabushita, S.; Zhang, Z. High-level multireference methods in the quantum-chemistry program system COLUMBUS: Analytic MR-CISD and MR-AQCC gradients and MR-AQCC-LRT for excited states, GUGA spin−orbit CI and parallel CI density. *Phys. Chem. Chem. Phys.* **2001**, *3*, 664−673.
(59) Lischka, H.; Müller, T.; Szalay, P. G.; Shavitt, I.; Pitzer, R. M.; Shepard, R. Columbus−a program system for advanced multireference theory calculations. *WIREs: Comp. Mol. Sci.* **2011**, *1*, 191−199.
(60) Lischka, H.; Shepard, R.; Shavitt, I.; Pitzer, R.; Dallos, M.; Müller, T.; Szalay, P.; Brown, F.; Ahlrichs, R.; Boehm, H. *COLUMBUS, an ab initio electronic structure program*, release 7.0; 2017.
(61) Lischka, H.; Shepard, R.; Müller, T.; Szalay, P. G.; Pitzer, R. M.; Aquino, A. J.; Araújo do Nascimento, M. M.; Barbatti, M.; Belcher, L. T.; Blaudeau, J.-P. The generality of the GUGA MRCI approach in COLUMBUS for treating complex quantum chemistry. *J. Chem. Phys.* **2020**, *152*, 134110.
(62) Gayvert, J. *OpenCAP*, Version 1.1.1; github, 2021. https://github.com/gayverjr/opencap.
(63) Hazi, A. U.; Rescigno, T. N.; Kurilla, M. Cross sections for resonant vibrational excitation of N_2 by electron impact. *Phys. Rev. A* **1981**, *23*, 1089.
(64) Meyer, H.-D. Optical potentials for electron-molecule scattering: A comparative study on the $N_2{}^2\Pi_g$ resonance. *Phys. Rev. A* **1989**, *40*, 5605.
(65) Sajeev, Y.; Santra, R.; Pal, S. Analytically continued Fock space multireference coupled-cluster theory: Application to the $^2\Pi_g$ shape resonance in e-N_2 scattering. *J. Chem. Phys.* **2005**, *122*, 234320.
(66) Zuev, D.; Jagau, T.-C.; Bravaya, K. B.; Epifanovsky, E.; Shao, Y.; Sundstrom, E.; Head-Gordon, M.; Krylov, A. I. Complex absorbing potentials within EOM-CC family of methods: Theory, implementation, and benchmarks. *J. Chem. Phys.* **2014**, *141*, No. 024102.
(67) Das, S.; Sajeev, Y.; Samanta, K. An Electron Propagator Approach Based on a Multiconfigurational Reference State for the Investigation of Negative-Ion Resonances Using a Complex Absorbing Potential Method. *J. Chem. Theory Comput.* **2020**, *16*, 5024−5034.
(68) Sommerfeld, T.; Santra, R. Efficient method to perform CAP/CI calculations for temporary anions. *Int. J. Quantum Chem.* **2001**, *82*, 218−226.
(69) Berman, M.; Estrada, H.; Cederbaum, L. S.; Domcke, W. Nuclear dynamics in resonant electron-molecule scattering beyond the local approximation: The 2.3-eV shape resonance in N_2^-. *Phys. Rev. A* **1983**, *28*, 1363.
(70) Feuerbacher, S.; Sommerfeld, T.; Santra, R.; Cederbaum, L. S. Complex absorbing potentials in the framework of electron propagator theory. II. Application to temporary anions. *J. Chem. Phys.* **2003**, *118*, 6188−6199.
(71) Ghosh, A.; Vaval, N.; Pal, S. Equation-of-motion coupled-cluster method for the study of shape resonance. *J. Chem. Phys.* **2012**, *136*, 234110.
(72) Thodika, M.; Fennimore, M.; Karsili, T. N.; Matsika, S. Comparative study of methodologies for calculating metastable states of small to medium-sized molecules. *J. Chem. Phys.* **2019**, *151*, 244104.
(73) Chao, J. S.; Falcetta, M. F.; Jordan, K. D. Application of the stabilization method to the N-2($1^2\Pi_g$) and Mg-(1^2P) temporary anion states. *J. Chem. Phys.* **1990**, *93*, 1125−1135.

https://doi.org/10.1021/acs.jctc.1c01096
J. Chem. Theory Comput. 2022, 18, 2863−2874